3D Target Simulations

W. Bo, R. Samulyak
SUNY Stony Brook
(March 3, 2009)

(1) Setup of the simulation.

The external energy deposition in the mercury jet is approximated by Sergei's calculation for a 24-GeV, 10-TP proton beam. His results can be found from the following website
http://www-ap.fnal.gov/~strigano/merit/edep_in_target/gravity/24gev-cir-gr/24gev-10t-circle-gr-10tp.out

In his results, the beam parameters $\sigma_x = 0.07894$ cm and $\sigma_y = 0.13394$ cm are used. No MHD processes are considered in our simulation. We study the hydrodynamic aspects of the problem. For the circular case, the radius of the jet is 0.795 cm. A mercury jet only 8-cm-long is simulated to save computational time. Only Sergei's data from z = 7 to 15 cm is used. See Fig 1 for the energy deposition at the initial time. The strong rarefaction waves result in cavitation bubbles. A discrete bubble insertion algorithm is used in the simulation with an initial bubble diameter 0.8 mm and bubble spacing 0.8 mm. The critical pressure for bubble insertion is -50 bar which is evaluated from thermodynamic equilibrium. The size of the computational domain is $3.5\,\text{cm} \times 3.5\,\text{cm} \times 10.5\,\text{cm}$ and the mesh is $100 \times 100 \times 300$.

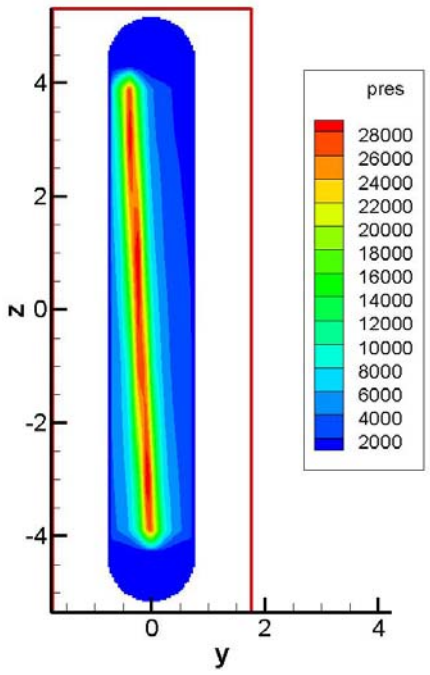

Fig 1. Sergei's energy deposition at the plane x = 0. The original results have units of Gev/gm/proton. Energy density has been converted to pressure (in bar) via the equation of state of mercury.

(2) Results and Conclusion

The jet surface and its interior cavitation structure at 160 μs are shown in Fig 2. The evolution of the interior is shown in Fig 3. The length and velocity of the two longest filaments are evaluated in Fig 4.

1. Due to the shape of the energy deposition, most filaments appear on the top surface ($y<0$) of the jet surface. Also, since the beam is longer in the y direction than in the x direction, the jet shows stronger perturbation in the y direction. This is consistent with the photos in the experiments.

2. Almost all cavitation bubbles appear during the propagation of the first rarefaction wave. See the left figure in Fig 3. This results in a 7% void fraction inside the jet. The expansion of the jet surface is mainly due to the expansion of these bubbles.

3. The filaments reach their maximal velocity when they first protrude out of the jet surface. Then the velocity decreases due to air resistance. Although filaments have different length, they expand at a similar speed at late times. The average filament velocity evaluated from the simulation is 35 m/s, less than Heejin's measurement for the corresponding case (45 m/s). There can be several reasons: First, the simulation has 40 cells across the jet diameter, the relatively coarse grid can introduce numerical diffusion which dumps the growth of the filaments. Second, the unknown parameters such as beam spot size the energy deposition at the viewpoint may affect observed velocity in the experiments. Last, there can be discrepancy between Sergei's results and the real energy deposition in the experiments.

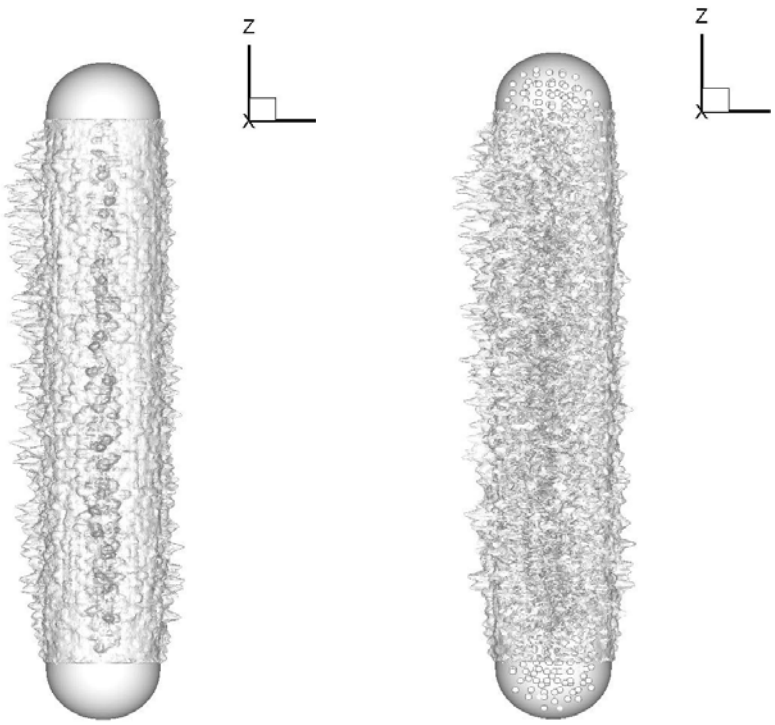

Fig 2. 160 μs after the interaction with proton beam. Left: the jet surface. Right: the cavitation inside the jet surface.

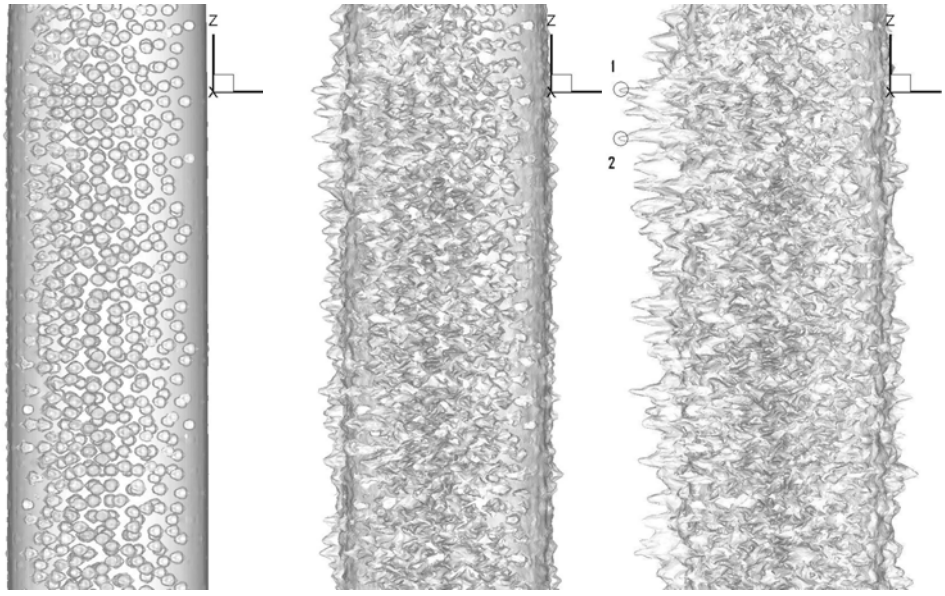

Fig 3. 13, 80, 160 μs after the interaction with proton beam, the jet segment from $0 < z < 4$ cm is shown.

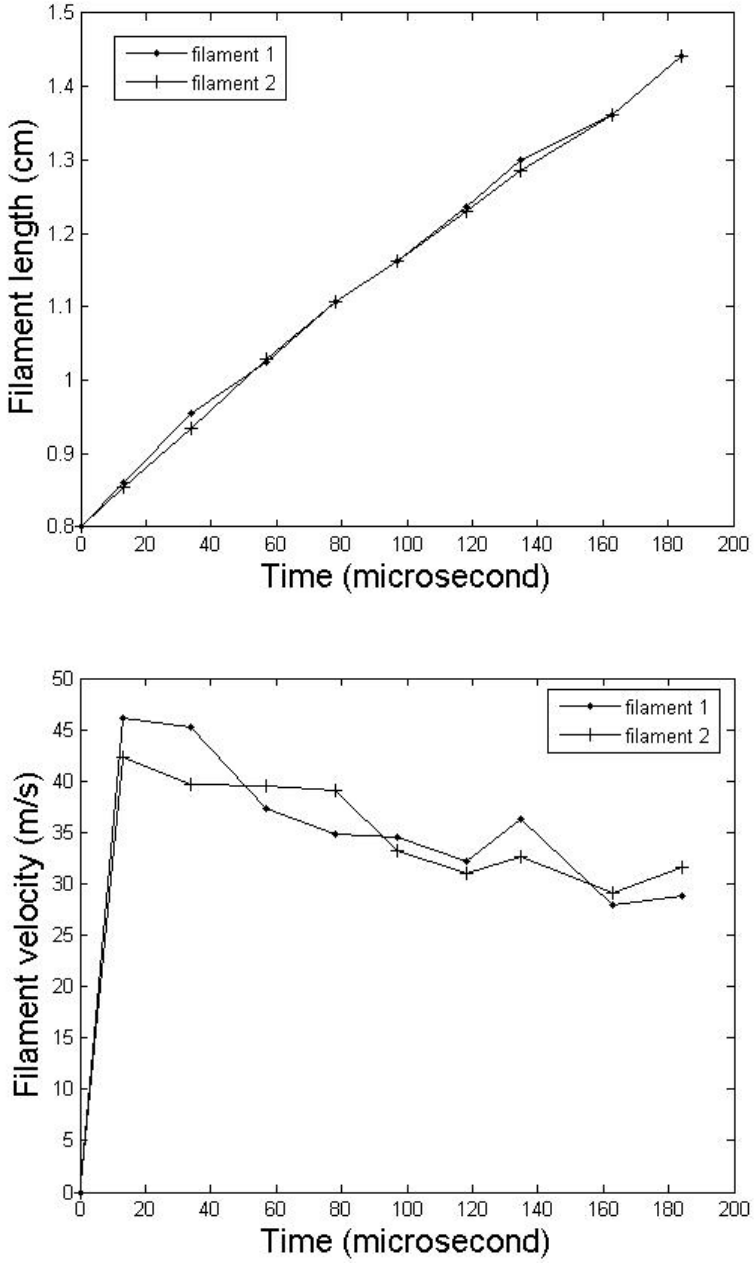

Fig 4. Time volution of filaments 1 and 2 in the right figure of Fig. 3. Upper: filament length *vs*. time. Lower: filament velocity *vs*. time.